

## Mechanical Stabilization Effect of Water on a Membrane-like System

Matteo Castronovo,<sup>†,‡</sup> Fouzia Bano,<sup>‡,§</sup> Simone Raugei,<sup>§,||</sup> Denis Scaini,<sup>†,‡</sup>  
Martina Dell'Angela,<sup>†,‡</sup> Robert Hudej,<sup>‡,§</sup> Loredana Casalis,<sup>‡</sup> and Giacinto Scoles<sup>\*,†,§,⊥</sup>

Contribution from the Physics Department, University of Trieste, P. Europa 1, 34127 Trieste, Italy, Elettra Synchrotron Laboratory, S.S.14 Km 163.5, 34012 Basovizza, Trieste, Italy, International School for Advanced Studies, Via Beirut 4, 34100 Trieste, Italy, and INFN Democritos Center, Via Beirut 4, 34100 Trieste, Italy

Received October 18, 2006; E-mail: gscoles@princeton.edu

**Abstract:** The penetration resistance of a prototypical model-membrane system (HS-(CH<sub>2</sub>)<sub>11</sub>-OH self-assembled monolayer (SAM) on Au(111)) to the tip of an atomic force microscope (AFM) is investigated in the presence of different solvents. The compressibility (i.e., height vs tip load) of the HS-(CH<sub>2</sub>)<sub>11</sub>-OH SAM is studied differentially, with respect to a reference structure. The reference consists of hydrophobic alkylthiol molecules (HS-(CH<sub>2</sub>)<sub>17</sub>-CH<sub>3</sub>) embedded as nanosized patches into the hydrophilic SAM by nanografting, an AFM-assisted nanolithography technique. We find that the penetration resistance of the hydrophilic SAM depends on the nature of the solvent and is much higher in the presence of water than in 2-butanol. In contrast, no solvent-dependent effect is observed in the case of hydrophobic SAMs. We argue that the mechanical resistance of the hydroxyl-terminated SAM is a consequence of the structural order of the solvent-SAM interface, as suggested by our molecular dynamics simulations. The simulations show that in the presence of 2-butanol the polar head groups of the HS-(CH<sub>2</sub>)<sub>11</sub>-OH SAM, which bind only weakly to the solvent molecules, try to bind to each other, disrupting the local order at the interface. On the contrary, in the presence of water the polar head groups bind preferentially to the solvent that, in turn, mediates the release of the surface strain, leading to a more ordered interface. We suggest that the mechanical stabilization effect induced by water may be responsible for the stability of even more complex, real membrane systems.

### Introduction

It is a matter of fact that the energetic stability of biological membranes is mediated by the presence of polar, hydrogen-bonding solvents and, in particular, of water. Nevertheless, a deeper understanding of the physical properties of these systems and, in particular, of the mechanical, as distinct from the energetic, stability, as they depend on the chemical nature of the solvent (e.g., water vs alcohol), is still missing. Atomic force microscopy (AFM) seems to be an almost ideal method to address such an issue. One of the limitations, however, in using AFM in situ on a real biological membrane is due to the relatively poor mechanical stability of cells and other similar systems such as liposomes and micelles as compared to the average force sensitivity of the AFM in liquid environments.<sup>1–5</sup> This difficulty can be overcome by using solid-supported

systems such as Langmuir-Blodgett monolayers or solid-supported lipid bilayers. Such layers are, however, not easily confined laterally as their molecules may “flow” laterally to escape the tip pressure, causing unwanted disruptions of the local membrane-like phase of the films.<sup>1,6–8</sup> To avoid this problem, self-assembled monolayers (SAMs) of thiols on gold (111) surfaces can effectively be used. In fact, by controlling the chemical nature of the terminal group of the molecules of a SAM, it is possible to impart completely hydrophilic character to the topmost interface of the SAM, obtaining in this way a model membrane system.<sup>8–11</sup> Moreover, the crystal-like order of the SAM<sup>12,13</sup> reduces the mobility of the molecules that start

<sup>†</sup> University of Trieste.

<sup>‡</sup> Elettra Synchrotron Laboratory.

<sup>§</sup> International School for Advanced Studies.

<sup>||</sup> INFN Democritos Center.

<sup>⊥</sup> Also affiliated with the Department of Chemistry and Princeton Materials Institute, Princeton University, Princeton, NJ 08544.

(1) Butt, H. J.; Cappella, B.; Kappell, M. *Surf. Sci. Rep.* **2005**, *59*, 1–152.

(2) Vinckier, A.; Semenza, G. *FEBS Lett.* **1998**, *430*, 12.

(3) Lehenkari, P. P.; Charras, G. T.; NykaKnen, A.; Horton, M. A. *Ultramicroscopy* **2000**, *82*, 289.

(4) Higgins, M. J.; Riener, C. K.; Uchihashi, T.; Sader, J. E.; McKendry, R.; Jarvis, S. P. *Nanotechnology* **2005**, *16*, S85.

(5) Higgins, M. J.; Polcik, M.; Fukuma, T.; Sader, J. E.; Nakayama, Y.; Jarvis, S. P. *Biophys. J.* **2006**, *91*, 2532.

(6) Santos, N. C.; Castanho, M. A. R. B. *Biophys. Chem.* **2004**, *107*, 133.

(7) Holden, M. A.; Jung, S. Y.; Yang, T.; Castellana, E. T.; Cremer, P. S. *J. Am. Chem. Soc.* **2004**, *126*, 6512.

(8) Hochrein, M. B.; Reich, C.; Krause, B.; Rädler, J. O.; Nickel, B. *Langmuir* **2006**, *22*, 538.

(9) Schwendel, D.; Hayashi, T.; Dahint, R.; Pertsin, A.; Grunze, M.; Steitz, R.; Schreiber, F. *Langmuir* **2003**, *19*, 2284.

(10) Houston, J. E.; Doelling, C. M.; Vanderlick, T. K.; Hu, Y.; Scoles, G.; Wenzl, I.; Lee, T. R. *Langmuir* **2005**, *21*, 3926.

(11) Pflaum, J.; Bracco, G.; Schreiber, F.; Colorado, R., Jr.; Shmakova, O. E.; Lee, T. R.; Scoles, G.; Kahn, A. *Surf. Sci.* **2002**, *498*, 89.

(12) Porter, M. D.; Bright, T. B.; Allara, D. L.; Chidsey, C. E. D. *J. Am. Chem. Soc.* **1987**, *109*, 3559.

(13) Camillone, N.; Chidsey, C. E. D.; Liu, G. Y.; Scoles, G. *J. Chem. Phys.* **1993**, *98*, 3503.

“flowing” at much higher forces exerted by the AFM tip. While this difference sets membrane-like SAMs further apart from the systems that we want to model, it has allowed us, as we hope to show below, to separate the mechanical stabilization effect of water on such systems from the purely energetic hydrophilic/hydrophobic stabilization that has been so far studied and understood much more extensively.

In this work, we focus on SAMs of hydroxyl-terminated alkylthiols HS-(CH<sub>2</sub>)<sub>11</sub>-OH (C11OH) on Au(111) films, which, like membranes, consist of hydrophobic chains and polar head groups. We have used contact mode AFM to study the compressibility of these SAMs in the presence of either water or, for comparison, 2-butanol as a function of the applied load. All measurements were taken differentially, using as a reference the behavior of 100 nm sized nanopatches of hydrophobic alkylthiols (HS-(CH<sub>2</sub>)<sub>17</sub>-CH<sub>3</sub> or C18) produced by nanografting.<sup>14–19</sup> Because the compressibility of a C18 patch is not expected to change significantly when measured in the presence of either water or 2-butanol as a function of the applied load, it can provide us with a reference behavior. By measuring side by side the relative height between C18 and C11OH, it is possible to measure the relative mechanical behavior of the two systems. We find that the mechanical resistance of the C11OH SAM in the presence of water is much higher than in the case of 2-butanol. This result is explained by showing through molecular dynamics simulations that the water molecules can mediate the interaction between the OH head-groups,<sup>10,11</sup> relaxing the surface strain present in the case of 2-butanol and allowing the SAM hydrocarbon chains to form a better ordered crystal.

## Experimental Section

Au(111) surfaces were produced by thermal evaporation of approximately 150 nm of gold at a rate of 0.02–0.03 nm/s at a background pressure of 10<sup>-8</sup> mbar on freshly cleaved mica substrates. The mica was first annealed for 24 h and then baked during the evaporation at 320 °C. Well-packed C11OH monolayers were obtained by immersing the Au(111) films into 100 μM solutions of 11-mercapto-1-undecanol (C11OH) (Sigma Aldrich, 97% purity), in absolute ethanol (Fluka, purity ≥99.8%), for at least 48 h.<sup>20</sup> Afterward, we confined 100 nm wide nanopatches of octadecanethiol [HS-(CH<sub>2</sub>)<sub>17</sub>-CH<sub>3</sub> or C<sub>18</sub>] SAMs, within the C11OH film, in correspondence of flat terraces, by using an AFM-based nanolithography technique called nanografting.<sup>14–19</sup> The protocol of nanografting involves scanning the tip of the AFM at a relatively large force (70–80 nN at 4 Hz) in the presence of a C18 solution, causing the thiols of the C11OH SAM to be replaced locally by C18 molecules. The AFM used in this work was a XE-100 microscope (Park Scientific Instruments Advanced Corp.), which mounts a custom liquid cell with an *xy* accessible area of 49.5 μm × 49.5 μm. All of the nanograftings and the other experiments were carried out using a silicon rectangular cantilever (MikroMasch, spring constant: 0.6–1.0 N m<sup>-1</sup>) freshly oxidized with piranha solution (sulfuric acid/hydrogen peroxide, 3/1, extremely oxidizing).

All of the measurements were taken within a few hours from the preparation of the patches to prevent SAM degradation. The compressibility measurements were carried out by scanning at constant speed (500 nm s<sup>-1</sup>) and load. The load was increased from the pull-off force

(referred as 0 nN) to approximately 70–80 nN at which a significant damage of the system was induced.

**Molecular Modeling Section.** The C11OH SAM was modeled as a two-dimensionally replicated patch of CH<sub>3</sub>(CH<sub>2</sub>)<sub>9</sub>CH<sub>2</sub>-OH molecules arranged according to a full-coverage of alkylthiols on Au(111) surface (with lattice constant *a* = 0.51144 nm). The simulations were carried out with the sander module of the Amber package,<sup>21</sup> using a stochastic Berendsen thermostat<sup>22</sup> to control the temperature and an integration time step for the equations of motion of 1.5 fs. The carbon atoms of the CH<sub>3</sub> ends were constrained according to a Au(111) surface. Simulations in water and 2-butanol were performed covering the monolayer, respectively, with a 3.5 nm- and a 8.0 nm-thick solvent layer (2769 and 1324 molecules, respectively). For both CH<sub>3</sub>(CH<sub>2</sub>)<sub>9</sub>CH<sub>2</sub>-OH and 2-butanol, the OPLS force field<sup>23</sup> was employed, whereas for water the SPC/E model<sup>24</sup> was used. All of the simulations were started with the alkylthiols oriented perpendicularly to the hypothetical gold surface. This configuration spontaneously evolves in a few tens of picoseconds into the (√3 × √3)R30° phase. During this time, the solvent promptly follows the monolayer reorganization. For both solvents, statistical analysis was performed on a 1 ns-long trajectory after an equilibration period of 0.5 ns. Starting from a different initial configuration or using a different water model leads substantially to the same results (see Figures SI.1 and SI.2 in the Supporting Information).

## Results and Discussion

**Mechanical Behavior of a Reference System.** Before showing and discussing our results, it is appropriate to discuss our expectations for the compressibility of the reference system. To understand the behavior of a system that like C18 is terminated with a hydrophobic group, we grafted C18 patches into a C10 SAM and measured the height difference as a function of the applied force in the presence of either 2-butanol or water. Both surfaces are hydrophobic, and the only difference between the patch and the SAM is the chain length of the molecules. Moreover, the chain length of C10 is very close to that of C11OH. A low load results in a height difference of 0.9 nm, while at higher load (>45 nN) the difference decreases (data not shown), regardless of the solvent used. This can be explained as follows: At low load, both the C18 and the C10 molecules are self-assembled, forming the typical alkylthiol low-energy hexagonal phase with the usual tilting angle of 30°–35° from the surface normal<sup>2,20</sup> (expected height difference 0.87 nm, in good agreement with the value reported above). As the load increases, if the height difference between the C18 and the C10 decreases, both of the films have to be necessarily compressed because it is highly unlikely that the longer chain system would collapse before the shorter one, which is energetically less stable.<sup>25</sup> The relative behavior between the C18 and C10 indicates that despite their different molecular lengths the two SAMs have the same mechanical resistance under the load of the AFM tip below 45 nN. This information significantly simplifies the study of the relative mechanical behavior of the C18/C11OH system, because it allows us to conclude that in the range of forces mentioned above the difference in molecular lengths between the two SAMs does not contribute to their relative mechanical resistance. Thus, we will be able to argue

(14) Xu, S.; Liu, G. Y. *Langmuir* **1997**, *13*, 127.

(15) Xu, S.; Laibinis, P. E.; Liu, G. Y. *J. Am. Chem. Soc.* **1998**, *120*, 9356.

(16) Xu, S.; Miller, S.; Laibinis, P. E.; Liu, G. Y. *Langmuir* **1999**, *15*, 7244.

(17) Liu, M.; Amro, N. A.; Chow, C. S.; Liu, G. Y. *Nano Lett.* **2002**, *2*, 863.

(18) Zhou, D.; Sinniah, K.; Abell, C.; Rayment, T. *Angew. Chem., Int. Ed.* **2003**, *42*, 4934.

(19) Case, M. A.; McLendon, G. L.; Hu, Y.; Vanderlick, T. K.; Scoles, G. *Nano Lett.* **2003**, *3*, 425.

(20) Ulman, A. *Chem. Rev.* **1996**, *96*, 1533.

(21) Case, D. A.; et al. *AMBER 7*; University of California, San Francisco, 2002.

(22) Berendsen, H. J. C.; Postma, J. P. M.; van Gunsteren, W. F.; DiNola, A.; Haak, J. R. *J. Chem. Phys.* **1984**, *81*, 3684.

(23) Jorgensen, W. L.; Maxwell, D. S.; Tirado-Rives, J. J. *J. Am. Chem. Soc.* **1996**, *118*, 11225.

(24) Berendsen, H. J. C.; Grigera, J. R.; Straatsma, T. P. *J. Phys. Chem.* **1987**, *91*, 6269.

(25) Fenter, P.; Eisenberger, P.; Liang, K. S. *Phys. Rev. Lett.* **1993**, *70*, 2447.

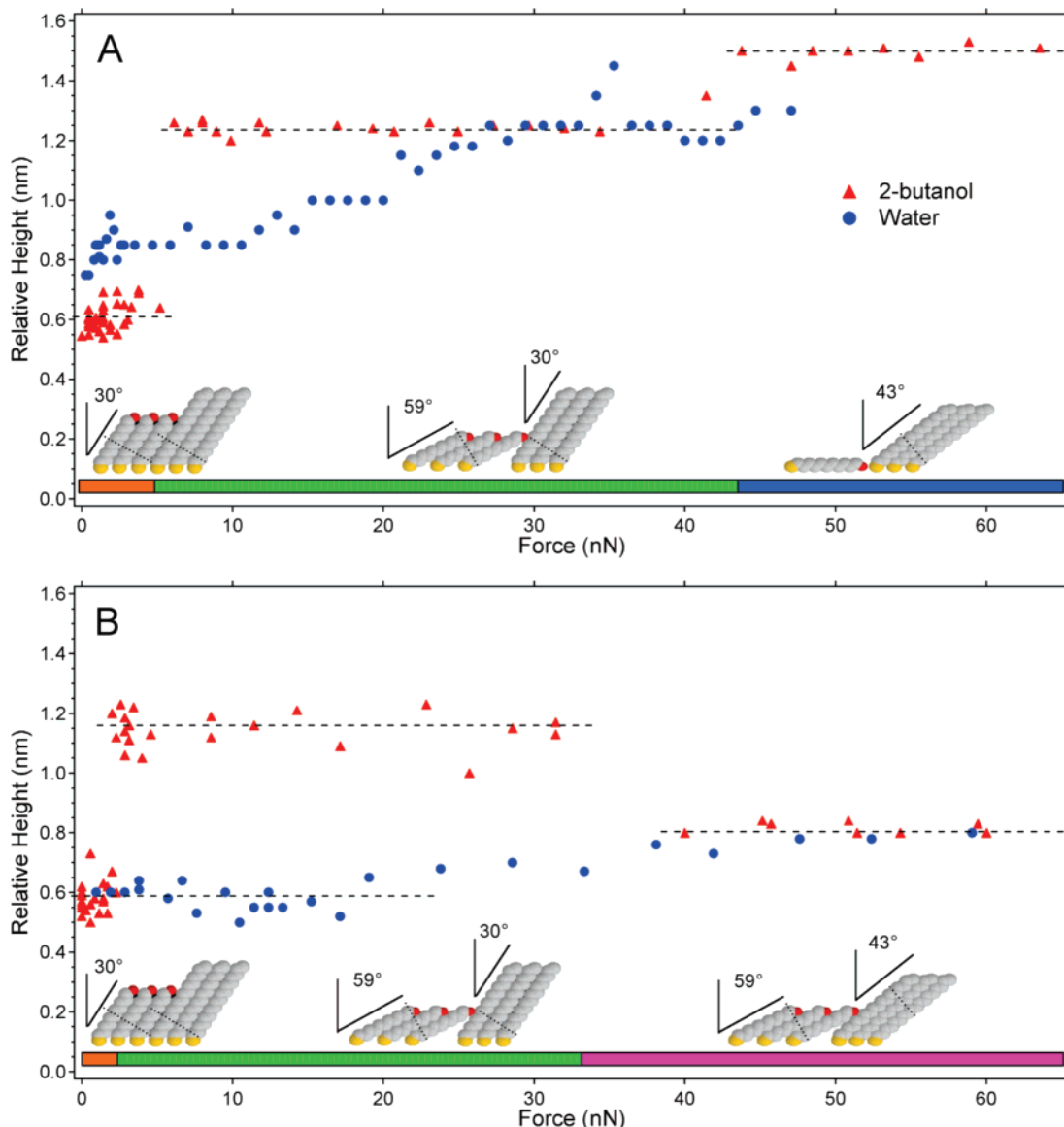


**Figure 1.** (A) Plots of the relative height between C18 patches and C11OH SAM versus applied load. (B) Plots of the relative height between C11OH patches and C18 SAM versus applied load. A molecular modeling of the system at different loads is shown at the bottom of both figures. In both systems, in the low force regime, the mechanical resistance of C11OH under the load of the AFM tip is greatly enhanced in the presence of water with respect to 2-butanol.

that the fact that in the presence of 2-butanol the height difference between patch and monolayer did sharply increase at very low values of the load instead of decreasing at much higher values (like in the case of the hydrophobic reference system, as will be shown below) can only be due to the hydrophilic termination of the C11OH SAM.

**AFM Results.** The results of a systematic study are reported in Figure 1A, where we show the plots of height difference versus force in the presence of the two solvents. Figure 2 shows two typical images with two typical height profiles.

In the presence of water, the relative height between C18 and C11OH slowly increases to reach the value of 1.2 nm at approximately 30 nN. This is to be contrasted with the fact that in the presence of 2-butanol a force threshold is found at 5 nN,

at which the relative height between the C18 and the C11OH changes in a single step from 0.6 to 1.2 nm. No hysteresis is found in this range of forces. As described above, because we do not expect the C18 layer to change its height below load values of 45 nN, the sudden increase in height difference, experienced in the presence of 2-butanol at approximately 5 nN, can only be explained as a lowering of the topmost layer of the C11OH SAM at that critical force value.

Stepwise changes of the height of SAMs under increasing tip loads have been previously reported by E. Barrena and co-workers.<sup>26,27</sup> They imaged at controlled relative humidity homogeneous nanoislands of methyl-terminated alkylthiols adsorbed on Au(111) films at a coverage below the full monolayer, measuring the absolute height of the patches as a function of the tip load. The interpretation of the discontinuous behavior of the height versus load curve was based on the fact that the hydrocarbon chains of the SAM are interlocked for

(26) Barrena, E.; Kopta, S.; Ogletree, D. F.; Charych, D. H.; Salmeron, M. *Phys. Rev. Lett.* **1999**, *82*, 2880.

(27) Barrena, E.; Ocal, C.; Salmeron, M. *J. Chem. Phys.* **2000**, *113*, 2413.

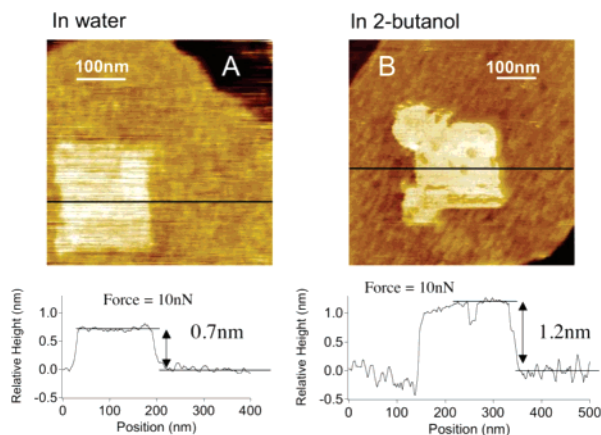


**Figure 2.** A patch of C18 grafted into the C11OH matrix on an atomically flat Au(111) terrace. Images are taken in the presence of water (A) and 2-butanol (B) at a force of 10 nN. In the case of water, the relative height measured between the C18 and the C11OH (see the profile in A) is approximately 0.7 nm. This value fits well with the one calculated by assuming that both C18 and C11OH are self-assembled in the unperturbed phase. In the case of 2-butanol, the relative height is about 1.2 nm, higher than in the case of water. Because the mechanical resistance of C18 is not likely to change as an effect of the solvent, the mechanical resistance of C11OH under the tip load should be lower in 2-butanol than in water.

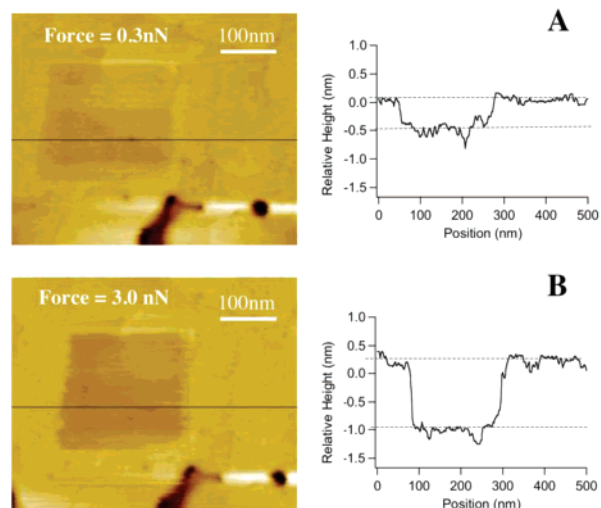


**Figure 3.** A patch of C11OH grafted into a C18 SAM. Both images are taken in the presence of 2-butanol at two different forces: (A) 0.3 nN and (B) 3.0 nN. This second value corresponds to the low force threshold in Figure 1B.

optimum Van der Waals interaction.<sup>28</sup> In principle, the interlocking condition can be satisfied only by certain tilting angles of the chains with respect to the surface normal. In turn, only certain values of the height of the SAM can be measured. Their results were explained by the fact that, under an increasing load, the tilting angle of the chains increases in single steps in correspondence with which the height of the SAM decreases. The expected angles of 43°, 55°, and 59° were shown to explain the plateaus of the height curve.<sup>27</sup>

In view of that work, our data can be interpreted as follows. In the presence of 2-butanol (see the scheme in Figure 1A), before the threshold at 5 nN, both the C18 and the C11OH molecules are tilted at 30°, being nearly unperturbed. The

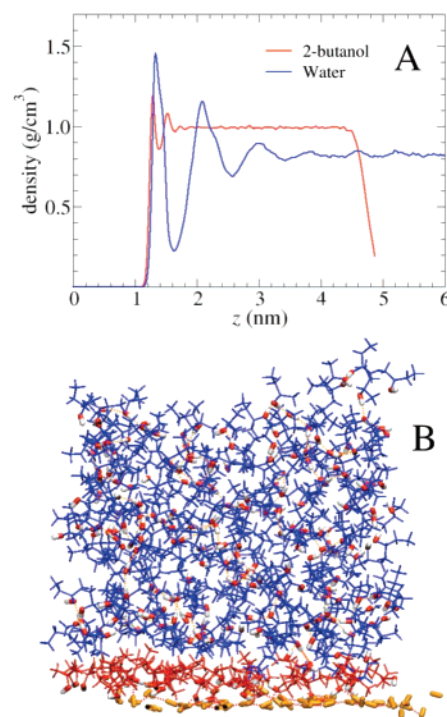


**Figure 4.** Molecular dynamics simulation results. (A) Density profiles of water (blue line) and 2-butanol (red line) shown as a function of the height above the C11OH SAM surface. (B) A schematic representation of a typical configuration of 2-butanol. The interactions between the first and second layer are mostly hydrophobic. In fact, the first layer of solvent (red sticks) strongly interacts with the monolayer OH heads (orange ellipses) and orients the apolar alkyl chains (red sticks) toward the bulk (blue sticks).

increase of the relative height above the threshold is due to a compression of the C11OH molecules (from 30° to 59°). Other important features in the relative height versus force behavior shown in Figure 2A are the ones described in what follows.

(1) In the presence of 2-butanol, the height difference remains constant at the value of ~1.2 nm between 5 and 45 nN; at 45 nN, a second threshold is found, and the height increases stepwise from 1.2 to 1.5 nm. This value can be explained by assuming that the C18 tilts to 43° while the C11OH is forced to the lying down phase.<sup>29</sup> At this point, the tip starts damaging the C11OH SAM, and thus the C11OH does not follow reversibly the height curve.<sup>14,26</sup> (2) In the presence of water, the relative height increases more or less continuously and slowly from 0.7 to 1.2 nm, in the range of forces between 0 and ~30 nN. The molecules of the C11OH SAM seem to tilt from 30° to ~59° under the increasing load of the tip by going through intermediate values that were not obtained in the presence of 2-butanol. For higher forces, the curves obtained in water and 2-butanol are similar. These findings prove that the mechanical stability of the C11OH SAM under the tip load is higher in the presence of water as opposed to 2-butanol and that such mechanical resistance is also always lower than for all methyl-terminated SAMs (e.g., C10 one and longer). The findings reported above were obtained for a patch of C18 into a C11OH SAM. The question that naturally arises is whether or not a patch of C11OH into a C18 SAM behaves in an equivalent way or at least similar. For that reason, we performed

(28) Outka, D. A.; Stöhr, J.; Rabe, J. P.; Swalen, J. D. *J. Chem. Phys.* **1988**, *88*, 4076.

(29) Munuera, C.; Barrena, E.; Ocal, C. *Langmuir* **2005**, *21*, 8270.

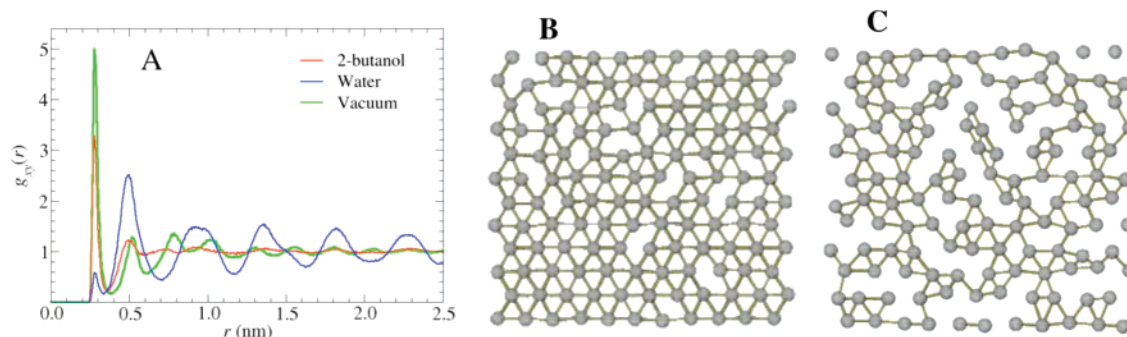


**Figure 5.** (A) In-plane oxygen–oxygen radial distribution functions (RDFs) in the C11OH SAM calculated in the presence of water (blue line), 2-butanol (red line), and in vacuum (green line). In the case of 2-butanol, the RDF is characterized by a marked first peak at 0.28 nm, which corresponds to a preferential formation of hydrogen bonds between the nearest-neighbor SAM heads, which is much higher than in the case of water. In the case of water, the regular sequence of peaks suggests a long-range  $(\sqrt{3} \times \sqrt{3})R30^\circ$  phase. These results are clearly understandable from (B) and (C), where the average monolayer oxygen-atom positions in the presence of water and 2-butanol, respectively, are shown; to better appreciate the level of order/disorder in the two solvents, atoms closer than 1.1 cell constants are connected by a line.

side by side compressibility experiments on nanopatches of C11OH grafted into C18 SAMs. Results are summarized in Figure 1B. In 2-butanol in the low force regime, the height difference behaves like in the reverse experiment, with evidence of a threshold at 3.0 nN. In Figure 3, two images, one below and one at the threshold load, are shown.

Two remarkable differences are found for forces higher than 20 nN. In the case of 2-butanol, the relative height decreases suddenly from nearly 1.2 to 0.8 nm at about 35 nN. This behavior can be explained by assuming that the C18 tilts to  $43^\circ$  (as found in the reverse experiment) while the C11OH remains tilted at  $59^\circ$ , never reaching the lying down phase found in the reverse experiment (see the scheme in Figure 1B). In the presence of water, the relative height remains constant at a mean value of 0.6 nm up to 20 nN of applied load, increasing gradually to reach the value of 0.8 nm at nearly 35 nN, corresponding to tilts of  $59^\circ$  and  $43^\circ$  for C11OH and C18, respectively. For higher loads, the behavior in the case of water is similar to that of 2-butanol.

The diverse behavior of the height difference curves between nanografting either the C18 or the C11OH that only apparently can be seen to complicate the data analysis will be discussed at the end of the paper after having understood, with the help of theory, the relationship between the molecular tilting and the order of the monolayer.

**Molecular Dynamics Simulations.** To rationalize the above-reported mechanical properties, molecular dynamics simulations of a model of C11OH SAM in water and 2-butanol were performed at room temperature. These simulations indicate that both solvents strongly interact via H-bonding with the OH monolayer heads. As a consequence, the solvent structure in the vicinity of the monolayer is largely perturbed. This is clearly indicated by the peaks present in the solvent density profiles reported in Figure 4A.

The perturbation extends to the second solvent layer in the case of water and to the third solvent layer in the case of 2-butanol. We also remark that the H-bonds between 2-butanol and monolayer are stronger than those between water and the

monolayer. This is suggested by longer H-bond average lifetimes ( $29 \pm 3$  ps vs  $17 \pm 1$  ps) and the more pronounced first minimum in the 2-butanol density profile. The analysis of the in-plane O–O radial distribution functions (RDFs), shown in Figure 5A, reveals marked differences between the SAM structures in the two solvents.

First, all of the RDFs are characterized by a first peak at 0.28 nm, which is due to the H-bonding between the nearest-neighbor SAM-heads. The number of such H-bonds decreases when going from the vacuum (also reported in Figure 5A) to 2-butanol and dramatically all but disappears in water. Second, while in the RDF relative to water the regular sequence of peaks, roughly spaced by a lattice constant, is suggestive of a long-range ordered  $(\sqrt{3} \times \sqrt{3})R30^\circ$  phase, in 2-butanol no long-range order is found. This different behavior can be understood in terms of different H-bonding patterns as follows. Because of the bulkier nature of 2-butanol, only few oxydriol groups face the SAM surface, and therefore the SAM is largely exposed to a hydrophobic environment (see Figure 4B). Hence, the polar head groups are mostly H-bonded to each other to minimize the head–head electrostatic interaction, as is also the case for the SAM in vacuum. Because of this inter-head H-bonding, any attempt to form an ordered  $(\sqrt{3} \times \sqrt{3})R30^\circ$  phase is necessarily obstructed by the incommensurability between the interacting dipole distances and the size of the aliphatic chains. Differently than 2-butanol, water has a size comparable to that of the SAM OH heads, and this guarantees that every SAM polar head has in average one water molecule to which to donate (and from which to receive) an H-bond. This allows for a decrease of the SAM surface strain and leads to a more ordered SAM phase.<sup>30</sup> The ordered and disordered nature of the  $(\sqrt{3} \times \sqrt{3})R30^\circ$  phases can be appreciated from Figure 5B and C, where a schematic representation of the average structure of the polar alkyl head sublattice, respectively, in water and 2-butanol is reported. We further remark that the nature of the disorder in 2-butanol is highly dynamical, with an average H-bonding lifetime of  $26 \pm 3$  ps, which should be compared to the average lifetime of the few interchain H-bonds present in water of  $16 \pm 1$  ps. It is also worth noticing that in 2-butanol the disorder largely extends up to C<sub>10</sub> and then rapidly decreases because of the tight chain packing.

(30) This finding is in accord with the trend previously reported by Sprik et al.: Sprik, M.; Delamarche, E.; Michel, B.; R othlisberger, U.; Klein, M. L.; Wolf, H.; Ringsdorf, H. *Langmuir* **1994**, *10*, 4116, who found a decreased number of head–head hydrogen-bonding interactions in 1:1 water-covered SH(CH<sub>2</sub>)<sub>11</sub>OH SAMs with respect to the dry monolayers.

Summarizing, atomistic simulations provide us with a simple macroscopic interpretation of the experimental results. In water, the release of the surface strain leads to an ordered C11OH SAM, which in turn increases the mechanical resistance of the monolayer.

**Differences in the Mechanical Behavior of C11OH as a SAM or as a Nanopatch.** Finally, we are addressing the different behavior between confining either the C18 or the C11OH molecules in the nanografted patch. We have solid evidence that the nanografting improves the molecular packing and reduces the density of defects in the nanografted patches with respect to the corresponding spontaneously adsorbed SAMs.<sup>31</sup> On the basis of this, we can now understand the two main differences between the curves in Figure 1A and B. Figure 1B represents the behavior of the height difference between a more compact C11OH phase (nanopatch) and a less compact C18 phase (monolayer). The difference in packing explains why the C18 molecules within the monolayer tilt to 43° at a force that is 10 nN lower than the force necessary to produce the same transition within the nanografted patch. This also explains why the C11OH molecules lie down horizontally at a higher force than the value that is found in Figure 1A. In the low force

range, we attribute the slightly earlier lowering of the C11OH from 30° to 59° to two factors: (1) the reproducibility of the measurements and (2) the fact that such tilting requires less extra space than the one from 59° to 90°. The behavior above 60 nN is irregular and not reported in the figures because it refers to the range of forces where the SAMs collapse under the load of the tip.

## Conclusions

This work demonstrates by AFM measurements and molecular dynamics simulations that the mechanical resistance to compression of a membrane-model system like a hydroxyl-terminated alkythiol SAM is affected by the presence of water. As opposed to 2-butanol, water is shown to relax the surface strain of the alcoholic interface of the SAM, leading to a phase of the SAM characterized by higher mechanical stability. Further work is necessary to find out if these results may also apply to real biological membranes. If this were to be the case, it would imply that the stabilizing action of water for biological membranes has a double nature.

**Acknowledgment.** We gratefully acknowledge fruitful discussions with Luis G. Rosa, Jian Liang, Fabian Herberg, and Francesco Stellacci.

**Supporting Information Available:** Monolayer in-plane oxygen–oxygen radial distribution functions calculated starting from a different initial configuration or using a different water model. Complete ref 21. This material is available free of charge via the Internet at <http://pubs.acs.org>.

JA067462I

(31) To confirm this, we performed side by side AFM friction measurements over nanopatches of thiols nanografted into SAMs of the same thiols (i.e., we performed autografting of C10, C14, C16, C18, and C11OH) and verified that the friction on the patches was always lower than that on the SAMs, in particular for the shorter thiols. On the other hand, the friction measured with the AFM is on average inversely proportional to the level of order of the SAM.<sup>10,11</sup>